Inorg. Chem. **2003**, *42*, 8557−8566

XAFS Studies of Anti-Inflammatory Dinuclear and Mononuclear Zn(II) Complexes of Indomethacin

Qingdi Zhou, Trevor W. Hambley,* Brendan J. Kennedy,* and Peter A. Lay*

Centre for Heavy Metals Research and Centre for Structural Biology and Structural Chemistry, School of Chemistry, The University of Sydney, Sydney NSW 2006, Australia

Received January 16, 2003

Zinc K-edge X-ray absorption fine structure (XAFS) experiments were performed in the solid and solution states at low temperature (10 K), on dimeric and monomeric anti-inflammatory Zn(II) complexes of indomethacin [1-(4-chlorobenzoyl)-5-methoxy-2-methyl-1*H*-indole-3-acetic acid = IndoH] of the formula $[Zn_2(Indo)_4L_2]$ [L = pyridine (Py), *N*,*N*-dimethylacetamide (DMA)], $[Zn(Indo)_2L_2]$ [L = ethanol (EtOH), methanol (MeOH)], and Zn(II) acetate dihydrate $[Zn(OAc)_2(OH_2)_2]$. The bond distances and angles obtained from multiple-scattering fits to the XAFS data of the Zn(II) dimeric complexes in the solid and solution states exhibit excellent correspondence with those obtained from single crystal diffraction studies. The Zn···Zn separations of 2.97 and 2.96 Å and carboxylato group O–C–O angles of 125° for powdered $[Zn_2(Indo)_4(Py)_2]$ and $[Zn_2(Indo)_4(DMA)_2]$ agree well with the XRD values of 2.969(1) and 2.9686(6) Å and 125.8(4)° and 126.1(2)°, respectively. The calculated Zn–O_{RCOO} and Zn–L bond distances of 2.03 and 2.04 Å, or 2.02 and 1.98 Å for Py or DMA complexes, respectively, also agree well with crystallographic data. The X-ray powder diffraction data on samples of the monomers exhibited additional reflections apart from those due to the crystallographically characterized *cis*-$[Zn(\eta^2\text{-}O,O'\text{-}Indo)_2L_2]$, but microanalyses were consistent with this formulation. Therefore, mixed models that contained the *cis* complex and a second component consisting of a *trans*-six-coordinate complex, a five-coordinate complex, or a four-coordinate complex were used to model the XAFS. The best fits to the XAFS data were obtained with a mixture of the *cis*-six-coordinate complex and a four-coordinate complex containing two monodentate Indo ligands. The bond lengths for the six-coordinate structure were consistent with those determined on a single crystal, and those for the four-coordinate complexes were consistent with related four-coordinate structures with two monodentate carboxylate ligands. Dissolution of the dimer (DMA adduct) in DMF resulted in a mixture of dimer and monomer species as shown by MS XAFS fitting. This is the first time that solution structures have been determined for anti-inflammatory Zn(II) complexes, and this is an important first step in understanding the pharmacology of the complexes.

Introduction

The nonsteroidal anti-inflammatory drug (NSAID) indomethacin [1-(4-chlorobenzoyl)-5-methoxy-2-methyl-1*H*-indole-3-acetic acid = IndoH] has been used for more then 30 years in the treatment of rheumatoid arthritis and other inflammatory or degenerative joint disorders.[1] As with most NSAIDs, indomethacin causes side effects such as headache, vertigo, etc. The most serious complication is gastrointestinal damage.[2,3] It is known that zinc and its complexes have gastroprotective effects against various ulcerogenic agents.[4] For instance, the zinc complexes of indomethacin and aspirin cause significantly less NSAID-induced gastric mucosal injury than do the parent NSAIDs.[5−7] This result indicates that the use of such zinc complexes as anti-inflammatory agents may be safer than the use of indomethacin or aspirin alone.

* To whom correspondence should be addressed. E-mail: t.hambley@chem.usyd.edu.au (T.W.H.); b.kennedy@chem.usyd.edu.au (B.J.K.); p.lay@chem.usyd.edu.au (P.A.L.).

(1) Abou-Mahamed, G.; El-Kashef, H. A.; Salem, H. A.; Elmazar, M. M. *Pharmacology* **1995**, *50*, 266−272.
(2) Wallace, M. S.; Zawie, D. A.; Garvey, M. S. *J. Am. Anim. Hosp. Assoc.* **1990**, *26*, 467−472.
(3) Ewing, G. O. *J. Am. Vet. Med. Assoc.* **1972**, *161*, 1665−1668.
(4) Joseph, R. M.; Varela, V.; Kanji, V. K.; Subramony, C.; Mihas, A. A. *Aliment. Pharmacol. Ther.* **1999**, *13*, 203−208.
(5) Singla, A. K.; Mediratta, D. K.; Pathak, K. *Int. J. Pharm.* **1990**, *60*, 27−33.
(6) Singla, A. K.; Wadhwa, H. *Int. J. Pharm.* **1994**, *108*, 173−185.
(7) Singla, A. K.; Wadhwa, H. *Int. J. Pharm.* **1995**, *120*, 145−155.

10.1021/ic034049s CCC: $25.00
Published on Web 11/14/2003

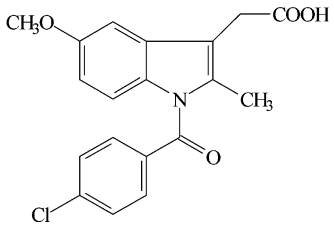

Indomethacin

Since zinc indomethacin complexes have anti-inflammatory properties and have been patented as veterinary pharmaceutics,[8] a number of Zn(II)−Indo complexes have been prepared and characterized.[9] Crystallographic studies show that the dimeric structures of $[Zn_2(Indo)_4L_2]$ (L = Py, DMA, NMP)[9] are similar to those found in $[Cu_2(Indo)_4L_2]$ (L = DMF, DMSO, DMA, THF, MeCN, Py),[10−12] except the Zn···Zn distance, where there is no bonding interaction, is much greater than the Cu−Cu distance, where there is a Cu−Cu bond. The monomer structures of *cis*-$[Zn(\eta^2\text{-}O,O'\text{-Indo})_2L_2]$ (L = EtOH, MeOH)[9] are similar to that of *cis*-$[Zn(OAc)_2(OH_2)_2]$.[13,14]

X-ray absorption fine structure (XAFS) has successfully been used in a number of cases to determine the coordination of metal ions and in the study of Cu(II)−Indo complexes.[15,16] The use of multiple-scattering (MS) techniques in the analysis of XAFS data gives information about the spatial arrangement of the atoms around the central absorber, for example, bond angles and distances.[17] In the present work, the solid- and solution-state Zn K-edge XAFS analyses of $[Zn_2(Indo)_4L_2]$ (L = Py, DMA), $[Zn(Indo)_2L_2]$ (L = EtOH, MeOH), and Zn(II) acetate dihydrate, $[Zn(OAc)_2(OH_2)_2]$ have been undertaken. The aim of this study was to examine whether the XAFS analysis could reproduce the geometry of the complexes observed in the crystal structures and hence be used to determine the structures of such species in pharmaceutical preparations and in solution, which is required for registration and understanding the pharmacology. The labile nature of the Zn complexes makes it difficult to determine the solution structures by other techniques, such as NMR spectroscopy, for instance, which gives the averaged structures.[9] It is essential to be able to determine the structures in solution because they have a marked effect on the gastric side effects of the Cu analogues, with dimers causing less gastrointestinal damage.[18]

Experimental Section

Complexes. The $[Zn_2(Indo)_4L_2]$ (L = Py, DMA) and $[Zn(Indo)_2L_2]$ (L = EtOH, MeOH) complexes were synthesized and characterized as reported previously.[9] $[Zn(OAc)_2(OH_2)_2]$ was obtained from Univar (99% purity).

Infrared Spectroscopy. Infrared spectra were recorded using a KBr matrix (400−4000 cm^{-1}) on a BIO-Rad Win-IR FTS-40 infrared spectrometer.

X-ray Powder Diffraction. X-ray powder diffraction data were collected at room temperature using Cu Kα radiation. The diffraction patterns were collected using a Shimadzu S6000 Diffractometer (40 kV, 30 mA, divergence and scatter slits 0.5°, and receiver slit 0.15 mm). The data were collected in the range 3−60° in steps of 0.02° in 2θ with a preset time of 15 s per step.

X-ray Absorption Spectra (XAS) Data Collection. The solid-state and solution Zn K-edge XAS data were collected at the Australian National Beamline Facility (ANBF), on bending magnet beamline 20B at the KEK Photon Factory, Tsukuba, Japan. The powdered samples were contained in Al cells (~1.0-mm thick) and were held in place by Kapton tape. Once the samples were mounted, they were immediately prechilled in liquid nitrogen prior to insertion into a Crydone REF-1577-D22 closed-cycle cryostat, and the temperature was maintained at 10 K with a Neocera LTC-11 temperature controller.

Data were collected under dedicated conditions at 2.5 GeV and 250−400 mA. A channel-cut Si(111) crystal was used as the monochromator. The X-ray absorption spectra for the solid samples were recorded in transmission mode at 10 K using standard N_2-filled ionization chambers. In order to reject most of the higher-order harmonics from the beam incident upon the sample, the monochromator crystal was detuned approximately 50% throughout the Zn K-edge XAFS measurements. To check for reproducibility and to improve counting statistics, at least three individual spectra were recorded for all powdered samples. The monochromator was calibrated to the first inflection point of a Zn foil (9660.0 eV).[19]

Fluorescence experiments were undertaken on the solution samples of $[Zn_2(Indo)_4(DMA)_2]$ and $[Zn(Indo)_2(EtOH)_2]$ in DMF at 10 K using a Canberra 10-element Ge detector in an experimental setup similar to that of the transmission mode, except the sample was orientated at 45° and the fluorescence was measured at 90° to the incidence beam. The solution samples contained 0.36% (w/w) of Zn for $[Zn_2(Indo)_4(DMA)_2]$ and 0.44% (w/w) of Zn for $[Zn(Indo)_2(EtOH)_2]$. Nine and five individual spectra were collected for $[Zn_2(Indo)_4(DMA)_2]$ and $[Zn(Indo)_2(EtOH)_2]$ in DMF solution, respectively.

The scans for each sample were averaged using weights based on the signal-to-noise ratios, and each XAFS spectrum was checked individually before averaging. A background correction was applied by fitting a single segment second-order polynomial to the pre-edge region, extrapolating it into the XAFS region, and subtracting it from the data. A three-region spline was fitted to the XAFS region and subtracted. The data were normalized to an edge jump of 1.0,

(8) Regtop, H. L.; Biffin, J. R. (Biochemical Veterinary Research Pty. Ltd., Australia) Divalent Metal Complexes of Indomethacin, Compositions and Medical Methods of Use Thereof. U.S. Patent 5466824, 1995.
(9) Zhou, Q.; Hambley, T. W.; Kennedy, B. J.; Lay, P. A.; Turner, P.; Warwick, B.; Biffin, J. R.; Regtop, H. L. *Inorg. Chem*. **2000**, *39*, 3742−3748.
(10) Weder, J. E.; Hambley, T. W.; Kennedy, B. J.; Lay, P. A.; MacLachlan, D.; Bramley, R.; Delfs, C. D.; Murray, K. S.; Moubaraki, B.; Warwick, B.; Biffin, J. R.; Regtop, H. L. *Inorg. Chem.* **1999**, *38*, 1736−1744.
(11) Weser, U.; Sellinger, K. H.; Lengfelder, E.; Werner, W.; Strahle, J. *Biochim. Biophys. Acta* **1980**, *631*, 232−245.
(12) Morgan, Y. R.; Turner, P.; Kennedy, B. J.; Hambley, T. W.; Lay, P. A.; Biffin, J. R.; Regtop, H. L.; Warwick, B. *Inorg. Chim. Acta* **2001**, *324*, 150−161.
(13) Van Niekerk, J. N.; Schoening, F. R. L.; Talbot, J. H. *Acta Crystallogr*. **1953**, *6*, 720−723.
(14) Ishioka, T.; Murata, A.; Kitagawa, Y.; Nakamura, K. T. *Acta Crystallogr., Sect. C* **1997**, *C53*, 1029−1031.
(15) Nagy, L.; Yamashita, S.; Yamaguchi, T.; Sipos, P.; Wakita, H.; Nomura, M. *J. Inorg. Biochem*. **1998**, *72*, 49−55.
(16) Weder, J. E.; Hambley, T. W.; Kennedy, B. J.; Lay, P. A.; Foran, G. J.; Rich, A. M. *Inorg. Chem.* **2001**, *40*, 1295−1302.
(17) Riggs-Gelasco, P. J.; Stemmler, T. L.; Penner-Hahn, J. E. *Coord. Chem. Rev*. **1995**, *144*, 245−286.
(18) Dillon, C. T.; Hambley, T. W.; Kennedy, B. J.; Lay, P. A.; Zhou, Q.; Davies, N. M.; Biffin, J. R.; Regtop, H. L. *Chem. Res. Toxicol.* **2003**, *16*, 28−37.
(19) George, G. N. *Centre for X-ray Optics X-ray Beamline Booklet*; SSRL: Berkeley, CA, 1993.

where the edge jump denotes the underlying intensity of the Zn-edge after subtracting the XAFS, and were compensated for decreasing absorbance past the edge. The background-subtracted, normalized, and compensated data were converted to *k*-space, where *k* is the magnitude of the photoelectron wave-vector and is related to the X-ray energy by the expression $k = \hbar^{-1}[2m_e(E - E_0)]^{1/2}$, where $\hbar$ is $h/2\pi$, m_e is the mass of the electron, E is the energy of the incident X-ray photon, and E_0 is the threshold energy for the removal of the core electron.[20]

XAS Data Analyses. The analyses of the XAFS data were performed by means of the program *XFIT*,[20] which uses nonlinear least-squares fitting to vary the model until the agreement between the observed and calculated XAFS is optimized. The XAFS of the model was calculated ab initio using the single-scattering (SS) program *FEFF* 4.06[21] or the curved-wave multiple-scattering (MS) XAFS program *FEFF* 6.01.[22] The parameters varied were the positions (*x*, *y*, *z*) of the atoms in the model in relation to an arbitrary set of Cartesian axes, the threshold energy (E_0), the scale factor (S_0^2), and the Debye−Waller factors (σ^2). The *k*-range used in the analysis of solid-state XAFS was 0−17.5 Å^{-1} for the SS and MS analyses, unless otherwise stated, while for the DMF solution samples of $[Zn_2(Indo)_4(DMA)_2]$ and $[Zn(Indo)_2(EtOH)_2]$ the XAFS *k*-spaces were 0−13.6 Å^{-1} and 0−13.4 Å^{-1}, respectively. The *k* and *r* windows used for the XAFS analyses are shown in the figures. The goodness-of-fit parameter R_{xafs} was calculated as described by Ellis and Freeman;[20] a R_{xafs} value of $\leq$ 20% is considered a good fit, and a R_{xafs} value of greater than 40% is poor.[23]

The degree of determinacy of the system for the fit (N_i/N_p)[23] was calculated from the number of independent data points (N_i) and the number of parameters (N_p), where if $N_i/N_p > 1$, the system is overdetermined and $N_i/N_p < 1$, the system is undetermined.[23] In the present work, the degrees of determinacy for the centrosymmetric MS models for dimeric and monomeric complexes were between 1.1 and 2.2.

The statistical errors in the final parameters arising from the noise in the data were estimated by Monte Carlo analysis.[20] The systematic errors (σ_s's) in the metal−nitrogen/oxygen bond lengths were assigned a conservative consensus value of 0.01−0.02 Å,[24] and combined with the Monte Carlo calculations of the random (statistical) errors (σ_r)[20] to obtain the estimated maximum root-mean-square (rms) error as $[(\sigma_r)^2 + (\sigma_s)^2]^{1/2}$.[25] The σ_s values for the bond angles were calculated using the estimated standard deviation (esd's) of the bond lengths and usually a σ_s value in a bond angle of 1° was calculated for a bond length with an esd of 0.02 Å.[16] The estimated maximum rms errors are shown in the present work as standard deviations in the reported bond lengths and angles.

SS XAFS Models. One-shell, five-coordinate single-scattering (SS) fits to the XAFS data for dimeric $[Zn_2(Indo)_4L_2]$ (L = Py, DMA), and two-shell, six-coordinate SS fits for monomeric $[Zn(Indo)_2L_2]$ (L = EtOH, MeOH) and *cis*-$[Zn(OAc)_2(OH_2)_2]$ were performed. The one-shell, five-coordinate SS model for the dimer comprised an oxygen scattering shell ($N_s = 5$) (four carboxylate oxygen atoms and one solvent ligand oxygen atom). For the monomer, the two-shell six-coordinate SS model comprised a carboxylate oxygen shell ($N_s = 4$) and a solvent ligand oxygen shell ($N_s = 2$).

For comparison with the results of the five-coordinate model of the dimeric complexes, a six-coordinate model was fitted. This model comprised a Zn scattering shell ($N_s = 1$) and an oxygen scattering shell ($N_s = 5$) (four carboxylate oxygen atoms and one solvent ligand oxygen atom). All SS analyses were undertaken without any constraints and restraints on the values for the threshold energy (E_0), scale factor (S_0^2), Debye−Waller factors (σ^2) and metal−ligand bond distances, unless otherwise stated.

MS XAFS Models. The MS models used for XAFS analyses of the Zn−Indo dimers and monomers are listed in Tables S1 and S2, respectively. The numbering systems for the models are given in Figures S1 and S2. The starting positional parameters of the MS models were taken from the crystal structural data of the Zn−Indo complexes.[9]

The MS fits were undertaken with constraints and restraints on certain parameters. All Debye−Waller factors, σ^2, were restrained to be positive and less than 0.02 Å^2 (or 0.01 Å^2 for the mixed model). The values of σ^2 were constrained to be the same for identical atoms in the model. The MS refinements included all non-hydrogen atoms of the solvent ligands. For the MS fits for the Zn dimers, 484 and 453 unique pathways were involved in the calculations for powdered $[Zn_2(Indo)_4(Py)_2]$ and $[Zn_2(Indo)_4(DMA)_2]$, respectively, where the total distance traveled by the photoelectron (R_{eff}) $\leq$ 10.2 Å and up to six legs were included. The MS fits for powdered monomeric $[Zn(Indo)_2L_2]$ and $[Zn(OAc)_2(OH_2)_2]$ complexes resulted in 71 (for L = EtOH), 64 (for L = MeOH), and 59 (for *cis*-$[Zn(OAc)_2(OH_2)_2]$) unique pathways with the total distance traveled by the photoelectron (R_{eff}) $\leq$ 9.0 Å and up to five legs. The MS paths and importance factors ($\geq$5%) for the dimeric and monomeric Zn complexes and $[Zn(OAc)_2(OH_2)_2]$ are given in Supporting Information (Tables S3−S7, respectively).

In addition, a mixed dimeric and monomeric model for a DMF solution sample of $[Zn_2(Indo)_4(DMA)_2]$ was investigated since the fits of the dimeric and monomeric models alone to the XAFS data for this sample were poor. In the mixed model, the two Zn absorber shells, one from each of dimeric, $[Zn_2(Indo)_4(DMF)_2]$, and monomeric, $[Zn(Indo)_2(DMF)_2]$, structures were placed 11 Å apart, which excluded their interactions during the modeling (maximal path length of a photoelectron was set at 5.1 Å). Conditions, restraints and constraints, applied to this mixed dimeric and monomeric model were similar to the corresponding single-phase dimeric or monomeric models. The occupancies (N_s) for all the atoms of the dimer and monomer were constrained to be equal with a weighting for the number of atoms of the same type. The sum of N_s (dimer) and N_s (monomer) was constrained to be equal to 1; the initial N_s values for all atoms were set at 0.5. The determinacy of the mixed models was ~1.1. The numbering system for the model is given in Figure S3.

The structural parameters obtained from fits of the *cis*-structure model to the XAFS data of Zn−Indo EtOH and MeOH complexes did not correspond well with the values from the previous crystal structural analysis. This is consistent with the X-ray powder diffraction patterns of these two complexes, which showed the presence of an additional crystalline phase in the bulk samples that was not that expected for a dimer. The microanalyses showed the sample to have the formula found in the crystal structure.[9] Hence, mixed models containing *cis*- and *trans*-$[Zn(\eta^2\text{-}O,O'\text{-Indo})_2L_2]$, or *cis*-$[Zn(\eta^2\text{-}O,O'\text{-Indo})_2L_2]$ with five- or four-coordinate monomers, were investigated.

(20) Ellis, P. J.; Freeman, H. C. *J. Synchrotron Radiat*. **1995**, *2*, 190−195.
(21) Mustre de Leon, J.; Rehr, J. J.; Zabinsky, S. I. *Phys. Rev. B.* **1991**, *44*, 4146−4157.
(22) Rehr, J. J.; Albers, R. C.; Zabinsky, S. I. *Phys. Rev. Lett*. **1992**, *69*, 3397−3401.
(23) Binsted, N.; Strange, R. W.; Hasnain, S. S. *Biochemistry* **1992**, *31*, 12117−12125.
(24) Gurman, S. J. *J. Synchrotron Radiat.* **1995**, *2*, 56−63.
(25) Rich, A. M.; Armstrong, R. S.; Ellis, P. J.; Freeman, H. C.; Lay, P. A. *Inorg. Chem*. **1998**, *37*, 5743−5753.

Table 1. Lattice Parameters and Selected Details of Refinements of the Powder Diffraction Patterns and Crystal Data for $[Zn_2(Indo)_4L_2]$ (L = Py, DMA) and $[Zn(Indo)_2(EtOH)_2]$

	Py		DMA		EtOH	
param	powder	cryst	powder	cryst	powder	cryst
space group	$P\bar{1}$ (No. 2)	$P\bar{1}$ (No. 2)	$P\bar{1}$ (No. 2)	$P\bar{1}$ (No. 2)	$C2/c$ (No. 15)	$C2/c$ (No. 15)
a (Å)	13.414(8)	13.347(3)	13.605(6)	13.628(2)	29.80(11)	30.086(2)
b (Å)	16.077(9)	16.499(5)	17.399(8)	17.462(2)	5.34(2)	5.3638(6)
c (Å)	10.907(7)	10.857(1)	11.057(5)	11.078(1)	22.86(10)	24.739(2)
α (deg)	98.82(3)	99.48(2)	99.44(2)	99.49(1)		
β (deg)	109.14(3)	108.25(2)	108.12(2)	108.13(1)	90.40(3)	90.342(7)
γ (deg)	105.21(3)	106.24(2)	109.91(2)	110.10(1)		

The mixed *cis*−*trans* isomer model included two Zn absorber shells, one for each of the *cis*-$[Zn(\eta^2\text{-}O,O'\text{-Indo})_2L_2]$ and *trans*-$[Zn(\eta^2\text{-}O,O'\text{-Indo})_2L_2]$ structures. The two Zn centers were placed 10 Å apart (maximal path length of a photoelectron was set at 4.5 Å) in order to ensure arbitrarily that there were no contributions from mutual interactions in the calculated XAFS. The conditions, restraints and constraints, applied to the mixed *cis*- and *trans*-models of $[Zn(\eta^2\text{-}O,O'\text{-Indo})_2L_2]$ were similar to those for the *cis*-$[Zn(\eta^2\text{-}O,O'\text{-Indo})_2L_2]$ model. The other mixed complex models used the same model for the *cis* complex but with five- or four-coordinate monomers as the other species. Preliminary work showed that only the four-coordinate complex fitted the second species, which was modeled using from the crystal structure of $[Zn(4\text{-}ClC_6H_4COO)_2(OH_2)_2]$ to obtain the starting coordinates.[26] The occupancies (N_s) for all the atoms of the *cis* complex with either *trans*-$[Zn(\eta^2\text{-}O,O'\text{-Indo})_2L_2]$ or the four-coordinate complex were constrained to be equal with a weighting for the number of atoms of the same type, and the sum of N_s (*cis*-isomer) and N_s (*trans*-isomer), or N_s (*cis*-isomer) and N_s (four-coordinate complex) was constrained to be equal to 1; the initial N_s values for all atoms were set at 0.5. The determinacy of the mixed models was ∼1.04.

Results

Infrared Spectroscopy. The IR spectra for the single crystal and bulk samples of $[Zn(Indo)_2(MeOH)_2]$ were almost the same (performed using the same batch of sample). Strong absorption peaks near 1580 and 1440 cm^{-1} corresponding to the asymmetric and symmetric carboxylato stretching frequencies, respectively, were obtained.[9] A small difference was observed for the carboxylate asymmetric stretching frequency $\nu_{as}(COO^-)$: for the single crystal, it appeared at 1587 cm^{-1}, while for the bulk sample it appeared at 1581 cm^{-1}.[27] The peak in the bulk sample is somewhat sharper.

X-ray Powder Diffraction. The lattice parameters obtained by powder X-ray diffraction studies of $[Zn_2(Indo)_4L_2]$ (L = DMA, Py) and $[Zn(Indo)_2L_2]$ (L = EtOH, MeOH) are listed in Table 1, along with the values obtained from single crystal methods. The powder diffraction pattern of $[Zn(Indo)_2(MeOH)_2]$ showed that only a small amount of the monoclinic ($C2/c$) phase identified in the single crystal XRD study was present. It was not possible to identify the crystal type of the major species present in the bulk sample, but it was established that this was not isostructural with the dimeric structure observed for $[Zn_2(Indo)_4(DMA)_2]$ and $[Zn_2(Indo)_4(Py)_2]$.

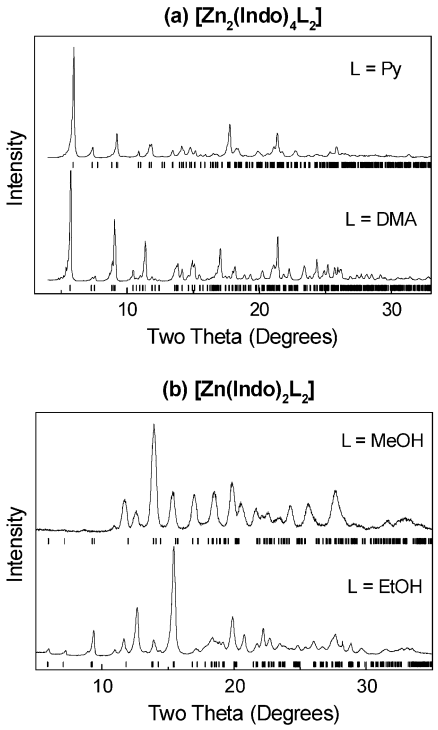

Figure 1. Powder X-ray diffraction patterns for (a) the dimeric $[Zn_2(Indo)_4L_2]$ (L = Py, DMA) and (b) the monomeric $[Zn(Indo)_2L_2]$ (L = EtOH, MeOH) complexes. In all cases, the short vertical marks give the positions of all of the Bragg reflections expected from the results of the single crystal analyses.

The powder XRD patterns of the two dimeric complexes were similar (Figure 1a) as expected for isostructural compounds. In both cases, the positions of the Bragg reflections calculated using the values obtained from the single crystal analyses were in good agreement with the observed positions. Importantly, no additional reflections were observed, which demonstrates that the single crystals used in the structural analyses were representative of the bulk samples in each case.

For the $[Zn(Indo)_2(EtOH)_2]$ complex, the single crystal *cis*-model accounted for many of the observed peaks; however, a small number of additional reflections were observed, most noticeably near $2\theta = 12.5°$ (Figure 1b). These additional peaks clearly demonstrate the presence of an additional crystalline phase.

For $[Zn(Indo)_2(MeOH)_2]$, additional reflections were observed near $2\theta = 12°$, and the expected peaks below 12° were very weak (Figure 1b). Further, all peaks in the powder pattern for L = MeOH were broader than those observed for the other complexes, indicating the sample was relatively

(26) Potocnák, I.; Dunaj-Jurco, M.; Cernák, J. *Acta Crystallogr., Sect. C* **1993**, *C49*, 1496−1498.
(27) Zhou, Q. Ph.D. Thesis, University of Sydney, 2001.

poorly crystalline. Although the nature of the other material in these monomeric samples has not been determined from powder diffraction, it clearly is not isostructural with the *cis*-$[Zn(\eta^2\text{-}O,O'\text{-Indo})_2(ROH)_2]$ structure identified in the single crystal XRD study, nor are the addition peaks due to the presence of dimeric complexes that are isostructural with $[Zn_2(Indo)_4L_2]$ (L = DMA, Py).

SS Analyses of the XAFS of Dimeric Zn−Indo Complexes. The results of SS fits to five- and six-coordinate models for powdered $[Zn_2(Indo)_4L_2]$ (L = Py, DMA) and a DMF solution of $[Zn_2(Indo)_4(DMF)_2]$ are given in Table S8, which includes the SS fitted bond distances (Å) and Debye−Waller factors (σ^2 (Å^2)) for Zn···Zn, mean Zn−O_{Ac}, and Zn−L. Detailed results are provided in the Supporting Information. The average Zn−O distances obtained for the dimers were within experimental error of the crystallographic values for a one-shell five-atom model or a two-shell model (five-oxygen-atom shell and one-zinc-atom shell). In the six-atom model, the Zn···Zn distance was also reproduced, but the fit was poorer than the five-atom model, showing SS analysis is not sufficient to distinguish a monomer from a dimer. SS analyses where also unsuitable for analyses of solutions of dimers (Supporting Information).

SS Analyses of the XAFS of Monomeric Zn−Indo Complexes. The fitting results of two-shell, six-coordinate SS models for powdered $[Zn(Indo)_2L_2]$ (L = EtOH, MeOH) and $[Zn(OAc)_2(OH_2)_2]$ samples, and for a DMF solution of $[Zn(Indo)_2(DMF)_2]$, are also shown in Table S8. The best fit of the unrestrained two-shell six-coordinate model to the XAFS data for powdered $[Zn(Indo)_2(EtOH)_2]$ resulted in Zn−O_{Ac} and Zn−L bond distances of 2.02(2) Å ($\sigma^2 = 0.003$ Å^2) and 1.94(2) Å ($\sigma^2 = 0.002$ Å^2), respectively ($R_{xafs} = 16.9\%$). These bond distances are shorter than the corresponding values determined in the crystal structure, of 2.178(3) and 2.015(3) Å.[9] The best fit to the unrestrained two-shell five-coordinate model (four-carboxylate-oxygen-atoms shell and one-solvent-ligand-atom shell) resulted in an unacceptably high Debye−Waller factor ($\sigma^2 = 0.92$ Å^2) for the Zn−O_{Ac} bond distance, and a unacceptably high scale factor ($S_0^2 = 3.30$). This indicates that the two-shell five-coordinate model does not adequately fit the XAFS data. Similar results were also obtained with these two models for the XAFS from Zn−Indo monomer in a DMF solution.

The fit to the XAFS data obtained from a solution of $[Zn(Indo)_2(DMF)_2]$ was also tested using the dimeric model. The best fit for the one-shell, five-coordinate model resulted in a mean Zn−O distance of 2.00(2) Å ($\sigma^2 = 0.009$ Å^2, $R_{xafs} = 20.5\%$). For the two-shell, six-coordinate model (one Zn-atom shell and one five-oxygen-atom shell), the fit was nonsensical because the Zn···Zn bond distance became negative.

Since the scale factor became very high (∼1.7) for the $[Zn(Indo)_2(MeOH)_2]$ complex in the unrestrained two-shell six-coordinate model fitting, a restraint on the scale factor of $S_0^2 \approx 0.9$ was used in a subsequent fitting to this model. The resultant mean Zn−O_{Ac} distance of 1.97(2) Å ($\sigma^2 = 0.004$ Å^2, $R_{xafs} = 21.6\%$) was shorter than the corresponding value of 2.173(3) Å determined from the crystal structure for the MeOH adduct.[9] However, the Zn−L bond distance of 2.03(2) Å ($\sigma^2 = 0.002$ Å^2) agreed well with the crystal structure value of 2.022(2) Å.[9] For the restrained two-shell five-coordinate model ($S_0^2 \approx 0.9$), the fit gave physically meaningless results as the Zn−O_{Ac} bond distance became negative. It is concluded that the complex does not have a five-coordinate geometry.

The best fit to the XAFS data obtained from powdered $[Zn(OAc)_2(OH_2)_2]$ was the two-shell, six-coordinate model, which resulted in a slightly shorter Zn−O_{Ac} bond distance of 2.11(2) Å ($\sigma^2 = 0.006$ Å^2) compared with those in the crystal structure of 2.184(4) Å in $[Zn(OAc)_2(OH_2)_2]$.[14] The Zn−O_{OH_2} bond distance of 1.98(2) Å ($\sigma^2 = 0.003$ Å^2) corresponded very well with the value from the crystal structure analysis.[14]

MS XAFS Analyses of Dimeric Zn−Indo Complexes. The MS fitting procedures for the XAFS from all the powdered and solution samples included all non-hydrogen atoms of the solvent ligand except atom C24 of the DMA in powdered $[Zn_2(Indo)_4(DMA)_2]$ (Figure S1b), C23 of the DMF in the solution sample $[Zn_2(Indo)_4(DMF)_2]$ (Figure S3a), and C38−C41 of the DMF in the solution sample $[Zn(Indo)_2(DMF)_2]$ (Figure S3b), which is ∼5.4 Å away from absorber atom Zn_0.[27] In order to reduce the number of independent variables in the fitting calculations, symmetry constraints were placed on all Zn−O and C−O bond distances in the carboxylato group, and on the C−C bond distances in the pyridine ring.

Table 2 lists XAFS parameters, selected bond distances, bond angles, and Debye−Waller factors obtained from the best MS fits to the XAFS data of powdered or solution $[Zn_2(Indo)_4L_2]$ (L = Py, DMA, DMF, Figure 2) samples. The XAFS (observed, calculated, and residual) and the corresponding Fourier transforms (FT) (observed, calculated, and residual) for the powdered $[Zn_2(Indo)_4(Py)_2]$ sample are shown in Figure 3. The MS refined Zn···Zn, mean Zn−O_{Ac}, and Zn−N_{Py} bond distances of 2.97(2) Å ($\sigma^2 = 0.003$ Å^2), 2.03(2) Å ($\sigma^2 = 0.006$ Å^2), and 2.04(2) Å ($\sigma^2 = 0.003$ Å^2), respectively, for the $[Zn_2(Indo)_4(Py)_2]$ complex are in excellent agreement with the respective crystallographic values of 2.969(1) Å, 2.039(2) Å, and 2.036(3) Å.[9] Similarly, the Zn···Zn, mean Zn−O_{Ac} and Zn−O_{DMA} bond distances of 2.97(2) Å ($\sigma^2 = 0.009$ Å^2), 2.02(2) Å ($\sigma^2 = 0.007$ Å^2), and 1.98(2) Å ($\sigma^2 = 0.003$ Å^2), respectively, in $[Zn_2(Indo)_4(DMA)_2]$ agree very well with corresponding values from the crystal structure, 2.9686(6) Å, 2.042(2) Å, and 1.989(2) Å.[9]

The Zn displacements from the least-squares plane through the square-pyramid-base of 0.38(2) Å for both of the powdered Py and DMA complexes are the same as the values from the crystal structures of 0.382(1) Å for the Py complex and 0.373(1) Å for the DMA complex.[9] The bridging O−C−O bond angles of the carboxylato groups for the powdered Py and DMA complexes (125(1)°) also correspond very well with those from the crystal structures of 125.8(4)° and 126.1(2)°, respectively.[9] The Zn···Zn···apex angles of 167(1)° and 174(1)° agree well with the crystal data of 166.93(9)° and 175.21(6)° for the Py and DMA complexes,

Table 2. Bond Distances (Å), Bond Angles (deg) and Debye−Waller Factors (σ^2 (Å^2)) of $[Zn_2(Indo)_4L_2]$ (L = Py, DMA) Obtained from the Best Fits of XAFS Data Using MS Analyses

complexes	bond angle O−C−O	bond distance Zn−Zn	bond distance Zn−O_{Ac}	bond distance Zn−L	Debye−Waller factor Zn−Zn	Debye−Waller factor Zn−O_{Ac}	Debye−Waller factor Zn−L	XAFS param E_0 (eV)	XAFS param S_0^2	XAFS param R_{xafs} (%)
$[Zn_2(Indo)_4(Py)_2]$[a]	125(1)	2.97(2)	2.03(2)	2.04(2)	0.003	0.006	0.003	−10.8	0.94	12.9
$[Zn_2(Indo)_4(Py)_2]$[b]	125.8(4)	2.969(1)	2.039(3)	2.036(3)						
$[Zn_2(Indo)_4(DMA)_2]$[a]	125(1)	2.97(2)	2.02(2)	1.98(2)	0.009	0.007	0.003	−8.2	0.90	16.6
$[Zn_2(Indo)_4(DMA)_2]$[b]	126.1(2)	2.9686(6)	2.042(2)	1.989(2)						
$[Zn_2(Indo)_4(DMF)_2]$[c]	125(1)	2.97(2)	2.06(2)	1.95(2)	0.02	0.008	0.01	−7.4	0.90	19.6
$[Zn(Indo)_2(DMF)_2]$[d]	119(1)		2.12(2)[g]	1.96(2)		0.012	0.002	−8.4	0.90	16.4
$[Zn_2(Indo)_4(DMF)_2]$[e]	126(1)	2.97(2)	2.01(2)	1.91(2)	0.01	0.002	0.006	−8.2	0.90	12.5
$[Zn(Indo)_2(DMF)_2]$[f]	120(1)		2.15(2)[g]	1.98(2)		0.007	0.003	−8.2	0.90	

[a] XAFS fitted data for the powdered samples (*k*-range: 0−17.5 Å^{-1}). [b] Crystal structure data.[9] [c] XAFS fitted data for the DMF solution sample (*k*-range: 0−13.6 Å^{-1}) using a dimeric model. [d] XAFS fitted data for the DMF solution sample (*k*-range: 0−13.6 Å^{-1}) using a monomeric model. [e] XAFS fitted data for the dimeric $[Zn_2(Indo)_4(DMF)_2]$ (37% of total Zn) in the mixed dimeric and monomeric model for a DMF solution sample of $[Zn_2(Indo)_4(DMA)_2]$. [f] XAFS fitted data for the monomeric $[Zn(Indo)_2(DMF)_2]$ (63% of total Zn) in the mixed dimeric and monomeric model for a DMF solution sample of $[Zn_2(Indo)_4(DMA)_2]$. [g] Mean Zn−O_{Ac} bond distance.

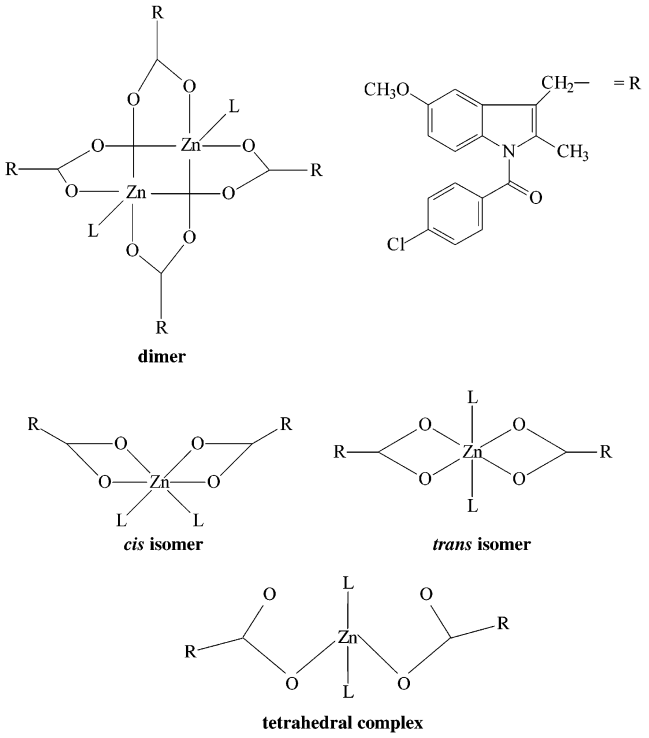

Figure 2. Structures of the Zn(II) complexes of Indo.

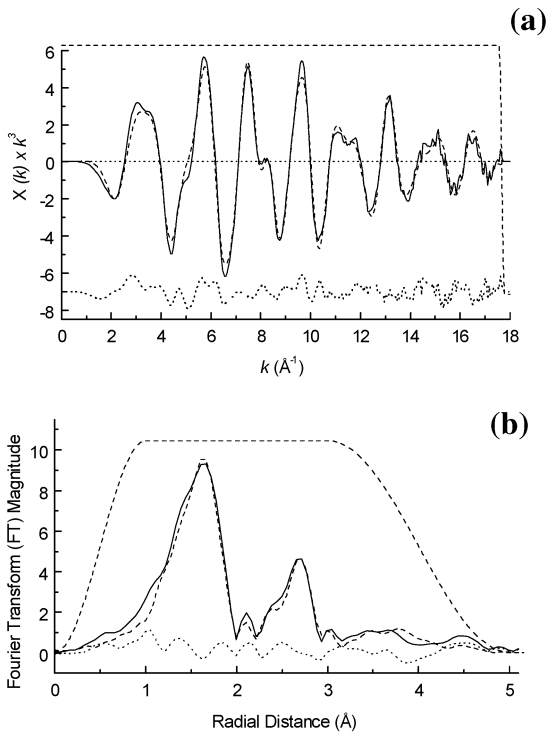

Figure 3. (a) Zn K-edge MS XAFS data, observed (—), calculated (- - -), and residual (···) for powdered $[Zn_2(Indo)_4(Py)_2]$ at 10 K. (b) Corresponding MS Fourier transform, observed (—), calculated (- - -), and residual (···) (R_{xafs} = 12.9%).

respectively. The lateral shift of the two zinc atoms, with respect to the principal dimer axis, of 0.35 and 0.15 Å obtained from the MS model fits for the powdered Py and DMA complexes are consistent with the crystal values of 0.34 and 0.13 Å. The R_{xafs} values of 12.9% and 16.6%, respectively, for the fits to the XAFS data of $[Zn_2(Indo)_4(Py)_2]$ and $[Zn_2(Indo)_4(DMA)_2]$ were good and overdetermined ($N_i/N_p \approx 1.1$).

For a DMF solution of $[Zn_2(Indo)_4(DMA)_2]$ in which the complex was modeled as $[Zn_2(Indo)_4(DMF)_2]$ (Table 2), the best MS XAFS fit to the data resulted in Zn···Zn, mean Zn−O_{Ac}, and Zn−O_{DMF} bond distances of 2.97(2) Å (σ^2 = 0.02 Å^2) and 2.06(2) Å (σ^2 = 0.008 Å^2) and 1.95(2) Å (σ^2 = 0.01 Å^2), respectively. These are in acceptable agreement with the values obtained for the solid-state sample in the crystallographic study. They were also similar to those obtained from the fit to the XAFS data for the powdered $[Zn_2(Indo)_4(DMA)_2]$ complex. The R_{xafs} value of 19.6% (N_i/N_p = 1.2) suggests that the dimeric model provides a reasonable fit to the XAFS data of solution $[Zn_2(Indo)_4(DMF)_2]$, but a monomer model was also tested.

The XAFS from the solution of $[Zn_2(Indo)_4(DMF)_2]$ was also fitted (Table 2) to the monomeric *cis*-Zn−Indo complex MS model (Figure 2) in order to determine whether the dimeric species is stable in solution. The best fit for the monomeric model resulted in Zn−O_{Ac} bond distances of 2.13(2) Å (σ^2 = 0.02 Å^2), and 2.10(2) Å (σ^2 = 0.004 Å^2), respectively, and Zn−O_{DMF} bond distance of 1.96(2) Å (σ^2 = 0.002 Å^2). The fitted bond distances were slightly shorter than the corresponding crystal structure values obtained from the *cis*-monomeric Zn(II)−Indo complexes.[9] The O−C−O bond angles of 119(1)° agreed well with the crystal value of ∼119° for $[Zn(\eta^2\text{-}O,O'\text{-Indo})_2(ROH)_2]$.[9] The

Table 3. Bond Distances (Å), Bond Angles (deg), and Debye−Waller Factors (σ^2 (Å^2)) Obtained from Fits to the XAFS Data for $[Zn(Indo)_2L_2]$ (L = EtOH, MeOH) and $[Zn(OAc)_2(OH_2)_2]$ Using Single-Site Models

complexes (coordination no.)	bond angle O−C−O	bond distance			Debye−Waller factor			XAFS param		
		Zn−O_{Ac}	Zn−O_{Ac}	Zn−L	Zn−O_{Ac}	Zn−O_{Ac}	Zn−L	E_0 (eV)	S_0^2	R_{xafs} (%)
$[Zn(Indo)_2(EtOH)_2]^a$ (6)	119.7(4)	2.183(3)	2.169(3)	2.015(3)						
cis-$[Zn(Indo)_2(EtOH)_2]^b$ (6)	117(1)	2.07(2)	2.04(2)	1.96(2)	0.02	0.004	0.003	−11.2	0.89	22.2
trans-$[Zn(Indo)_2(EtOH)_2]^c$ (6)	117(1)	2.08(2)	2.04(2)	1.96(2)	0.02	0.003	0.002	−10.8	0.89	21.5
$[Zn(Indo)_2(EtOH)_2]^d$ (4)	120(1)	1.98(2)		1.98(2)	0.005		0.004	−15.7	0.90	18.6
$[Zn(Indo)_2(MeOH)_2]^a$ (6)	119.4(4)	2.195(3)	2.151(3)	2.022(3)						
cis-$[Zn(Indo)_2(MeOH)_2]^b$ (6)	117(1)	2.07(2)	2.04(2)	1.96(2)	0.02	0.002	0.002	−8.7	0.90	24.1
trans-$[Zn(Indo)_2(MeOH)_2]^c$ (6)	117(1)	2.08(2)	2.04(2)	1.96(2)	0.02	0.002	0.002	−8.7	0.90	23.8
$[Zn(Indo)_2(MeOH)_2]^d$ (4)	120(1)	2.03(2)		1.95(2)	0.001		0.002	−11.9	0.90	15.4
$[Zn(OAc)_2(OH_2)_2]^a$ (6)	117.5(5)	2.189(4)	2.179(4)	1.987(4)						
$[Zn(OAc)_2(OH_2)_2]^b$ (6)	119(1)	2.19(2)	2.15(2)	2.00(2)	0.019	0.005	0.004	−11.4	0.91	17.8
cis-$[Zn(Indo)_2(DMF)_2]^e$ (6)	118(1)	2.12(2)	2.09(2)	1.96(2)	0.017	0.002	0.002	−9.6	0.91	20.8
trans-$[Zn(Indo)_2(DMF)_2]^f$ (6)	118(1)	2.11(2)	2.08(2)	1.96(2)	0.012	0.005	0.004	−9.4	0.91	27.3
$[Zn(Indo)_2(DMF)_2]^g$ (4)	119(1)	1.94(2)		2.07(2)	0.002		0.002	−15.6	0.90	35.2

[a] Crystal structural data for *cis*-Zn complexes with bidentate carboxylato groups.[9,14] [b] Fits of XAFS data to the *cis*-model for powdered samples. [c] Fits of XAFS data to the *trans*-model for powdered sample. [d] Fits of XAFS data to the four-coordinate model for powdered samples (these can be compared with the Zn−O_{Ac} = 1.991(5) Å, Zn−O_L = 1.973(5) Å, and ∠O−C−O = 119.7(6)° values in the crystal structure of $[Zn(4\text{-}ClC_6H_4COO)_2(H_2O)_2]$).[26] [e] Fits of XAFS data to the *cis*-model for the solution sample (in DMF). [f] Fits of XAFS data to the *trans*-model for the solution sample (in DMF). [g] Fits of XAFS data to the four-coordinate model for the solution sample (in DMF).

goodness-of-fit parameter, R_{xafs} = 16.4% (N_i/N_p = 1.2), was quite good, and much better than the fit to the dimeric model of 19.6%. This result is consistent with the results obtained from the SS analyses. It showed that the monomeric DMF-complex model was more consistent with the XAFS data for a DMF solution sample of $[Zn_2(Indo)_4(DMA)_2]$ and suggested that a substantial amount of the initially formed dimeric $[Zn_2(Indo)_4(DMF)_2]$ complex converted into the monomeric DMF species in solution. Since both models provided acceptable fits but did not result in exceptionally good fits to the XAFS obtained for $[Zn_2(Indo)_4(DMA)_2]$ in DMF, a mixed dimeric and monomeric model was examined (Table 2, Figure 4). The Zn···Zn and Zn−O_{Ac} bond distances of 2.97(2) Å (σ^2 = 0.01 Å^2) and 2.01(2) Å (σ^2 = 0.002 Å^2) for dimeric $[Zn_2(Indo)_4(DMF)_2]$ obtained from the mixed model corresponded very well with those obtained from the crystal structure values.[9] The Zn−O_{DMF} distance of 1.91(2) Å (σ^2 = 0.006 Å^2) was significantly shorter than the corresponding X-ray structural value of 1.989(2) Å for Zn−O_{DMA}.[9] The Zn−O_{Ac} and Zn−O_{DMF} bond distances of 2.15-(2) Å (σ^2 = 0.007 Å^2) and 1.98(2) Å (σ^2 = 0.003 Å^2) for monomeric $[Zn(Indo)_2(DMF)_2]$ in the mixed model agreed well with the crystal structure values for $[Zn(\eta^2\text{-}O,O'\text{-}Indo)_2(ROH)_2]$.[9] The R_{xafs} value of 12.5% (N_i/N_p = 1.1) indicated the fit was very good. The occupancies (N_s) for the atoms of the dimer and monomer Zn−Indo complex in the DMF solution were 0.37 and 0.63, respectively. This indicates that the dimers were substantially converted to the monomer in the 5.2% (w/w) DMF solution.

MS XAFS Analyses of Monomeric Zn−Indo Complexes. The best MS fits to the XAFS data of powdered samples of $[Zn(Indo)_2L_2]$ (L = EtOH, MeOH) and $[Zn(OAc)_2(OH_2)_2]$ using a *cis*, *trans*, or four-coordinate model (Figure 2) are given in Table 3. The MS fits for the data for the two monomeric complexes, $[Zn(\eta^2\text{-}O,O'\text{-}Indo)_2(EtOH)_2]$ and $[Zn(\eta^2\text{-}O,O'\text{-}Indo)_2(MeOH)_2]$, using a *cis* model resulted in much higher R_{xafs} values than those obtained in fits to the dimeric complexes discussed earlier, and there was poor agreement of the calculated bond length related to those from

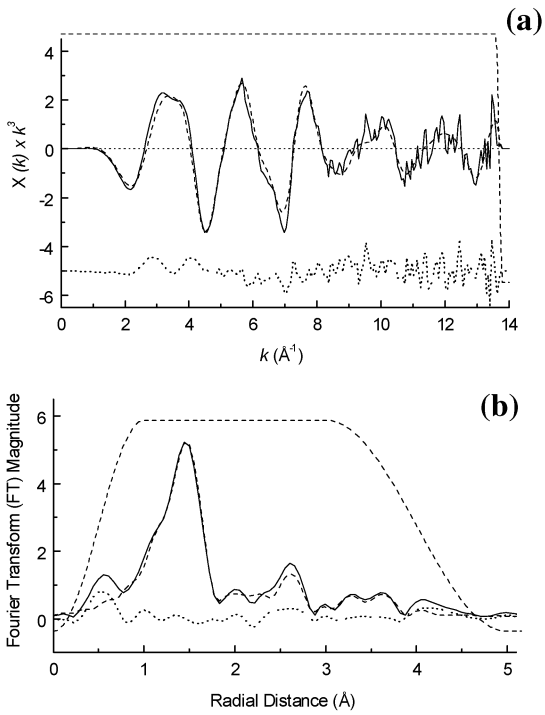

Figure 4. (a) Zn K-edge MS XAFS data, observed (—), calculated (- - -), and residual (···) for a frozen DMF solution sample of $[Zn_2(Indo)_4(DMA)_2]$ at 10 K using the mixed dimeric and monomeric model. (b) Corresponding MS Fourier transform, observed (—), calculated (- - -), and residual (···) (R_{xafs} = 12.5%).

the single crystal analyses. For example, the best fit to the $[Zn(Indo)_2(EtOH)_2]$ XAFS data gave mean Zn−O_{Ac} and Zn−O_{EtOH} bond distances of 2.06(2) and 1.95(2) Å (R_{xafs} = 19.6%, N_i/N_p = 1.2), respectively, which are significantly shorter than the corresponding values obtained from diffraction analysis, i.e., 2.176(3) and 2.015(3) Å.[9] Similar results were obtained in attempts to fit the XAFS data for $[Zn(Indo)_2(MeOH)_2]$ to the *cis*-model or for the $[Zn(Indo)_2L_2]$ (L = EtOH, MeOH) complexes to a *trans*-model (Table 3). For both complexes, much better fits were obtained to a tetrahedral four-coordinate model (Figure 2) in which both the Indo ligands were monodentate (Table 3). The average

Table 4. Fitted Bond Distances (Å), Bond Angles (deg), and Debye−Waller Factors (σ^2 (Å^2)) for the Mixed Models of [Zn(Indo)$_2$L$_2$]

complex	bond angle O−C−O	bond distances (Å)			Debye−Waller factor			XAFS param			
		Zn−O_{Ac}	Zn−O_{Ac}	Zn−L	Zn−O_{Ac}	Zn−O_{Ac}	Zn-L	N_s[d]	E_0 (eV)	S_0^2	R_{xafs} (%)
cis-[Zn(Indo)$_2$(EtOH)$_2$][a]	120(1)	2.20(2)	2.17(2)	2.01(2)	0.01	0.01	0.001	0.38	−9.9	0.90	16.3
trans-[Zn(Indo)$_2$(EtOH)$_2$][a]	120(1)	2.08(2)	1.99(2)	1.93(2)	0.001	0.001	0.002	0.62	−9.9	0.90	
cis-[Zn(Indo)$_2$(EtOH)$_2$][a]	120(1)	2.19(2)	2.16(2)	1.97(2)	0.01	0.01	0.001	0.17	−12.4	0.90	13.7
4-coord [Zn(Indo)$_2$(EtOH)$_2$][a,b]	120(1)	1.95(2)		2.04(2)	0.002		0.002	0.83	−12.4	0.91	
cis-[Zn(Indo)$_2$(DMF)$_2$][c]	119(1)	2.19(2)	2.15(2)	2.00(2)	0.013	0.004	0.002	0.49	−9.1	0.90	20.6
trans-[Zn(Indo)$_2$(DMF)$_2$][c]	117(1)	2.08(2)	2.03(2)	1.93(2)	0.001	0.004	0.001	0.51	−9.1	0.91	
cis-[Zn(Indo)$_2$(DMF)$_2$][c]	120(1)	2.12(2)	2.10(2)	1.95(2)	0.009	0.004	0.003	0.77	−9.5	0.91	24.7
4-coord [Zn(Indo)$_2$(DMF)$_2$][a,b]	120(1)	1.97(2)		2.03(2)	0.004		0.001	0.23	−9.5	0.90	
cis-[Zn(Indo)$_2$(MeOH)$_2$][a]	120(1)	2.20(2)	2.18(2)	1.97(2)	0.01	0.01	0.001	0.31	−8.3	0.90	19.2
trans-[Zn(Indo)$_2$(MeOH)$_2$][a]	120(1)	2.06(2)	2.02(2)	1.94(2)	0.002	0.002	0.002	0.69	−8.3	0.90	
cis-[Zn(Indo)$_2$(MeOH)$_2$][a]	120(1)	2.20(2)	2.17(2)	1.95(2)	0.01	0.01	0.001	0.12	−11.0	0.90	13.8
4-coord [Zn(Indo)$_2$(MeOH)$_2$][a,b]	120(1)	1.95(2)		2.04(2)	0.002		0.001	0.88	−11.0	0.91	

[a] Fits to the mixed-isomer model to the XAFS data for powdered samples. [b] Four-coordinate monodentate Zn carboxylate. [c] Fits to the mixed-isomer model to the XAFS data for a DMF solution sample. [d] Occupancies for *cis*, *trans*, or four-coordinate isomer.

Zn−O bond lengths of 1.98 and 1.99 Å for L = MeOH and EtOH, respectively, are as expected for four-coordinate complexes, such as the model complex [Zn(4-ClC_6H_4COO)$_2$(H$_2$O)$_2$], where it is 1.98 Å.[26]

The single crystal XRD structure of [Zn(OAc)$_2$(OH$_2$)$_2$] has previously been determined by Van Niekerk et al.[13] and Ishioka et al.[14] This compound has a six-coordinate *cis* geometry similar to those found for [Zn(η^2-*O*,*O*′-Indo)$_2$(EtOH)$_2$] and [Zn(η^2-*O*,*O*′-Indo)$_2$(MeOH)$_2$].[9] The MS fits to the XAFS data for [Zn(OAc)$_2$(OH$_2$)$_2$] using the *cis*-model resulted in mean Zn−O_{Ac} and Zn−O_{OH_2} bond distances of 2.17(2) Å (σ^2 = 0.012 Å^2) and 2.00(2) Å (σ^2 = 0.004 Å^2), respectively, which are in good agreement with the distances reported previously, 2.184(4) and 1.987(4) Å, respectively.[14] The fitted bond angle of the carboxylato group O−C−O of 119(1)° and the chelate bite angle O−Zn−O of 60(1)° are also similar to the literature values of 117.5(5)° and 59.0(1)°.[14] These values together with the R_{xafs} value of 17.8% and the determinacy of the fit, 2.2, clearly demonstrate the *cis* model is reasonable for the XAFS of [Zn(OAc)$_2$(OH$_2$)$_2$] and shows that the poor fit of the *cis* model to the XAFS data of the alcohol complexes was not due to problems with the model.

The MS fitting to the XAFS data for [Zn(Indo)$_2$(EtOH)$_2$] in DMF solution using a monomeric *cis*-[Zn(η^2-*O*,*O*′-Indo)$_2$(DMF)$_2$] model gave a mean Zn−O_{Ac} bond distance of 2.11(2) Å (Table 3), that is 0.05 Å longer than that of the XAFS-derived value of 2.06(2) Å obtained from a powdered sample of [Zn(Indo)$_2$(EtOH)$_2$], and 0.07 Å shorter than crystal structure value (2.176 Å).[9] The Zn−O_{DMF} = 1.96(2) Å distance obtained from the model fit was similar to that found for the Zn−O_{EtOH} bond in the fit to the data obtained from a powdered [Zn(Indo)$_2$(EtOH)$_2$] sample. The R_{xafs} value of 19.9% (N_i/N_p = 1.5) showed that the fit was acceptable and much better than the four-coordinate model, but the weighted average bond length of 2.06 Å is too small to be consistent with the presence of only an octahedral complex. Hence, a dimeric [Zn$_2$(Indo)$_4$(DMF)$_2$] model was also investigated. The best fit for the model gave a greater R_{xafs} value of 28.8% (N_i/N_p = 1.2). The Zn···Zn vector distance of 2.97(2) Å (σ^2 = 0.02 Å^2), mean Zn−O_{Ac} = 2.05(2) Å (σ^2 = 0.008 Å^2), and Zn−O_{DMF} = 1.93(2) Å (σ^2 = 0.009 Å^2) were similar to those obtained from the dimeric model fit to the data from solid state [Zn$_2$(Indo)$_4$(DMA)$_2$]. While the bond lengths are more reasonable than those obtained for the monomer models, the poor R_{xafs} value showed that the dimeric model is unsatisfactory and shows that it cannot be the only species in solution.

As described previously, the powder XRD patterns for the two monomeric Zn−Indo complexes showed additional reflections that were not predicted from the results of the single crystal XRD structure. The microanalyses showed the sample to have the formula found in the crystal structure, demonstrating that a second phase of similar formula was present. The IR spectra from the same batch of material in the single crystal analysis and bulk sample of [Zn(Indo)$_2$(MeOH)$_2$] were very similar. A small difference was observed for carboxylate asymmetric stretching frequency ν_{as}(COO$^-$) ($\Delta\nu$ = 6 cm^{-1}). Accordingly, a model consisting of a mixture of *cis*- and *trans*-[Zn(η^2-*O*,*O*′-Indo)$_2$L$_2$] (L = EtOH, MeOH) was investigated. When such a mixed model was used, the resultant mean Zn−O_{Ac} bond distance of 2.19(2) Å (σ^2 = 0.01 Å^2) and Zn−O_{EtOH} bond distance of 2.01(2) Å (σ^2 = 0.005 Å^2) for the *cis* isomer of [Zn(η^2-*O*,*O*′-Indo)$_2$(EtOH)$_2$] and mean Zn−O_{Ac} distance of 2.19(2) Å (σ^2 = 0.01 Å^2) and Zn−O_{MeOH} bond distance of 1.97(2) Å (σ^2 = 0.001 Å^2) for the *cis* isomer of [Zn(η^2-*O*,*O*′-Indo)$_2$(MeOH)$_2$] were obtained, which are in very good agreement with the respective crystal structure values of 2.176(3) and 2.015(3) Å for the EtOH complex, and to a lesser extent, the corresponding values of 2.174(3) and 2.022(2) Å in the MeOH complex. The carboxylato O−C−O bond angle of 120(1)° and the chelate bite angle O−Zn−O of 60(1)° for the *cis*-isomers of both the EtOH and MeOH complexes obtained from the mixed model fits were also in excellent agreement with the crystal structural values of ∼119.5° and ∼60.1°, respectively.[9] The R_{xafs} values of 16.3% (N_i/N_p = 1.04) for the EtOH complex and 19.2% (N_i/N_p = 1.02) for the MeOH complex indicated that the fits were good. Table 4 lists the bond distances and angles obtained from the best fits of the mixed *cis*- and *trans*-model for the [Zn(η^2-*O*,*O*′-Indo)$_2$L$_2$] complexes.

The fitted mean Zn−O_{Ac} and Zn−L bond distances for the *trans*-isomer, obtained from the mixed model fits, of ∼2.04(2) and ∼1.93(2) Å for [Zn(η^2-*O*,*O*′-Indo)$_2$(EtOH)$_2$] and [Zn(η^2-*O*,*O*′-Indo)$_2$(MeOH)$_2$] were shorter than those

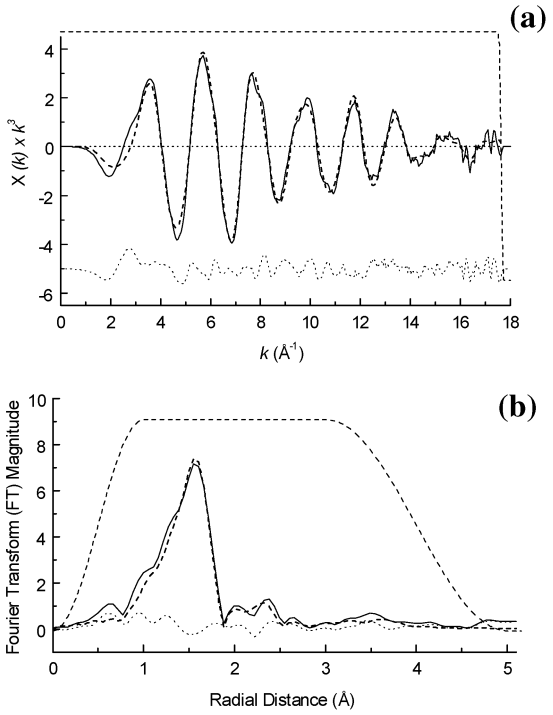

Figure 5. (a) Zn K-edge MS XAFS data, observed (—), calculated (- - -), and residual (···) for fitting of the mixed *cis* and four-coordinate model to XAFS data of a powdered sample of $[Zn(Indo)_2(EtOH)_2]$ at 10 K. (b) Corresponding MS Fourier transform, observed (—), calculated (- - -), and residual (···) (R_{xafs} = 13.7%).

obtained from the *cis*-isomers, and the average Zn−O bond length (2.00−2.01 Å) was much shorter than that expected for six-coordinate Zn(II) (2.12 Å in each of the three XRD structures in Table 3). The carboxylato O−C−O bond angle of ∼115(1)° was also smaller than that found in the *cis*-isomer. The fitted occupancies (N_s) for the atoms of *cis*- and *trans*-$[Zn(\eta^2\text{-}O,O'\text{-}Indo)_2L_2]$ were 0.34 and 0.66 when L = EtOH, and 0.31 and 0.69 when L = MeOH.

Since the four-coordinate model gave a better fit to the XAFS than either of the *cis* or *trans* six-coordinate complexes in the single-site models, a mixed model containing the *cis*-octahedral and the tetrahedral complexes was also examined. Such models resulted in much better fits to the XAFS data and more reasonable bonding parameters. The average bond lengths for the six-coordinate complexes (2.11 Å) and four-coordinate complexes (1.99_5 Å) were the same as related crystallographically characterized complexes, and the lower contributions of the *cis*-octahedral complex to the XAFS compared to the previous mixed-site model is consistent with the powder XRD results. The XAFS and the corresponding Fourier transforms (FT) for the mixed-isomer model fits to the XAFS data of powdered $[Zn(Indo)_2(EtOH)_2]$ are shown in Figure 5, and the bond length and angle data are contained in Table 4.

The fits of the mixed *cis*- and *trans*-model to the XAFS data of solution $[Zn(\eta^2\text{-}O,O'\text{-}Indo)_2(DMF)_2]$ was also investigated. The best fit for the *cis* isomer yielded mean Zn−O_{Ac} and Zn−O_{DMF} distances of 2.16(2) Å (σ^2 = 0.004 Å^2) and 1.97(2) Å (σ^2 = 0.001 Å^2), and O−C−O and O−Zn−O angles of 119(1)° and 61(1)° (Table 4). The best fit for the *trans*-isomer in the mixed model for the solution $[Zn(\eta^2\text{-}O,O'\text{-}Indo)_2(DMF)_2]$ resulted in mean Zn−O_{Ac} and Zn−O_{DMF} bond distances of 2.06(2) Å (σ^2 = 0.001 Å^2) and 1.92(2) Å (σ^2 = 0.001 Å^2), and O−C−O and O−Zn−O bond angles of 117(1)° and 63(1)°. However, the average bond length of 2.01 Å for the *trans* isomer is too small for an octahedral complex, and the weighted average Zn−O bond length of the two isomers (2.06 Å) is too short for the data to be consistent with only a monomer in solution. The weighted average bond length is closer to that expected for a dimer of 2.03−2.04 Å (Table 2). The occupancies (N_s) for the atoms of the mixed *cis*- and *trans*-$[Zn(\eta^2\text{-}O,O'\text{-}Indo)_2(DMF)_2]$ model were 0.44 and 0.56 (R_{xafs} = 17.9%, N_i/N_p = 1.04).

Since the weighted average bond length was closer to that expected for a dimer, the solution sample was also tested using a mixed monomeric and dimeric model. A higher R_{xafs} value of 24.0% from the best fit was obtained. A mixed model that incorporated both the *cis* octahedral complex and a four-coordinate complex also resulted in a worse fit to the data.

Discussion

The use of SS analyses of the XAFS data confirmed the presence of a similar dimeric coordination environment for powdered $[Zn_2(Indo)_4L_2]$ (L = Py, DMA) samples and in a solution sample of $[Zn_2(Indo)_4(DMF)_2]$, but such analyses were unable to reproduce accurately the bond distances about the Zn sites. For example, the distances to the axial ligands were poorly reproduced, probably because the two independent bond distances Zn−L and Zn−O_{Ac} were too similar. The difference between the axial and equatorial Zn−O distances is only 0.003 and 0.053 Å for the Py and DMA complexes, respectively,[9] which is much less than the minimum resolution of different shells obtained from Fourier theory,[28,29] $\pi/2\Delta k_{max}$ = 0.089 Å, where Δk_{max} is the *k*-range used in the XAFS refinement, in this case 17.5 Å^{-1}. The SS model fits for the XAFS data from the powdered samples of monomeric $[Zn(Indo)_2L_2]$ (L = EtOH, MeOH) and a solution sample of $[Zn(Indo)_2(DMF)_2]$ are similar, and the fitted Zn−O_{Ac} bond distances, are 0.12−0.20 Å shorter than the crystal structure values.[9]

The use of MS models in the analyses of the XAFS data for the dimeric Zn complexes was successful. The fitted bond lengths and angles for the powdered $[Zn_2(Indo)_4L_2]$ (L = Py, DMA) samples are in excellent agreement with those obtained from the single crystal structure analyses. The bond distances and angles obtained from the best fit for the dimeric model for XAFS from a DMF solution sample of $[Zn_2(Indo)_4(DMA)_2]$ (containing 0.36% (w/w) of Zn, and assuming the DMF substituted for DMA) are also consistent with the crystal structure values. Interestingly, the monomeric *cis*-model also fitted the data from the solution sample of $[Zn_2(Indo)_4(DMF)_2]$. The fitted mean Zn−O_{Ac} and Zn−L bond distances agreed well with the values obtained from a single

(28) Penner-Hahn, J. E. *Coord. Chem. Rev.* **1999**, *190*−*192*, 1101−1123.
(29) Lee, P. A.; Citrin, P. H.; Eisenberger, P.; Kincaid, B. M. *Rev. Mod. Phys.* **1981**, *53*, 769−807.

crystal XRD investigation of *cis*-[Zn(η^2-*O*,*O*′-Indo)$_2$(ROH)$_2$].[9] The R_{xafs} value for the fit to the monomer model (16.4%) is better than for the dimer model (19.6%). Using the mixed dimer and monomer model to fit the data resulted in an even better fit with bond length values that agree well with the respective crystal structure values. The results of allowing the relative amounts of the components to vary during the fitting procedure indicate that the DMF solution contains about 37% dimer. However, the exact proportions of monomer and dimer are not determined accurately because of the lower *k*-range of the solution data compared to the solid state data. The results do show, however, that the complex partially dissociates to form an equilibrium mixture that contains dimeric and monomeric species. The results obtained from solution studies on the monomeric [Zn(Indo)$_2$-(EtOH)$_2$] complex in DMF are more difficult to interpret, since the best fit to the data is with a monomer, but the bond lengths are more consistent with the predominance of a dimer. The ambiguity probably arises from the quality of the data, which is poorer than that obtained for a solution of the dimer, which causes the low level of determinacy to be a more important issue. It is revealing that the intensity of the peak at ~2.5 Å with respect to the main peak in the Fourier transform is similar for DMF solutions of both the dimer and the monomer (Figures S6 and S7). By contrast, this peak, which is mainly due to the second Zn atom in dimers, is very weak in the monomers in the solid state (Figure 5). These factors taken together are consistent with a mixture of monomer and dimer in DMF, irrespective of whether the complex that was dissolved was a monomer or dimer. These conclusions are consistent with recent results obtained by ^{1}H NMR diffusion experiments, which indicate that dissolving either a monomeric or a dimeric complex in DMF results in mixtures of the two complexes, since the diffusion coefficient is higher than for dimeric Cu(II) complexes.[30]

MS XAFS analyses cannot reproduce the monomeric *cis*-[Zn(η^2-*O*,*O*′-Indo)$_2$L$_2$] (L = EtOH, MeOH) structures since additional phases, seen in the powder XRD studies, are present. On the basis of a comparison with the powder XRD analyses of dimeric Zn−Indo and Cu−Indo complexes,[10] no reflections indicative of a dimeric structure were observed in the powder diffraction patterns for the monomeric *cis*-[Zn(Indo)$_2$L$_2$] (L = EtOH, MeOH) complexes. The best XAFS fits are obtained when the additional phase was modeled as the tetrahedral complex with two monodentate Indo ligands. Such a model not only gave the best fit but gave the correct bond lengths for the octahedral and tetrahedral complexes in the mixture. In addition, the amounts of the *cis*-octahedral components in this model were less than in the optimized models in which the components were modeled as mixtures of *cis* and *trans* geometric isomers. This result is also consistent with the low amounts of *cis*-[Zn(Indo)$_2$(ROH)$_2$] deduced from the powder diffraction experiments.

(30) Ramadan, S.; Hambley, T. W.; Kennedy, B. J.; Lay, P. A. To be submitted.

Acknowledgment. The authors gratefully acknowledge the support of this work from the Australian Research Council (ARC), Biochemical Veterinary Research Pty Ltd and Nature Vet Pty Ltd for a SPIRT grant and an ARC RIEFP grant for the Ge fluorescence detector. X-ray absorption spectroscopy was performed at the Australian National Beamline Facility with support from the Australian Synchrotron Research Program, which is funded by the Commonwealth of Australia under the Major National Research Facilities Program. The authors also gratefully acknowledge Drs. Garry Foran and James Hester for assistance at ANBF and Dr. Jane Weder for her continual willingness to help during the course of the XAFS data analysis. Q.Z. acknowledges funding of an ARC Australian Postgraduate Research Award (Industry).

Supporting Information Available: MS models used for XAFS analyses for Zn−Indo dimers and monomers; the MS paths and importance factors contributing to the XAFS model refinement of all powdered samples; SS fitting parameters and results for Zn−Indo dimers and monomers; MS fitting parameters for all XAFS models; figures of the atomic numbering system for dimeric, monomeric, and mixed models; and figures of the Zn K-edge XAFS data and the corresponding Fourier transforms for powdered [Zn$_2$(Indo)$_4$(DMA)$_2$], [Zn(OAc)$_2$(OH$_2$)$_2$], and a solution sample of [Zn(Indo)$_2$(DMF)$_2$]. This material is available free of charge via the Internet at http://pubs.acs.org.

IC034049S